ACS APPLIED MATERIALS & INTERFACES

Research Article

Cite This: ACS Appl. Mater. Interfaces 2019, 11, 40260−40266

www.acsami.org

Redox-Inactive CO_2 Determines Atmospheric Stability of Electrical Properties of ZnO Nanowire Devices through a Room-Temperature Surface Reaction

Kentaro Nakamura,[†] Tsunaki Takahashi,*[,†] Takuro Hosomi,[†] Takehito Seki,[‡] Masaki Kanai,[†] Guozhu Zhang,[†] Kazuki Nagashima,[†] Naoya Shibata,[‡] and Takeshi Yanagida*[,†]

[†]Institute for Materials Chemistry and Engineering, Kyushu University, 6-1 Kasuga-Koen, Kasuga, Fukuoka 816-8580, Japan

[‡]Institute of Engineering Innovation, The University of Tokyo, 2−11−16 Yayoi, Bunkyo, Tokyo 113−8656, Japan

Supporting Information

ABSTRACT: Emerging interactive electronics for the Internet of Things era inherently require the long-term stability of semiconductor devices exposed to air. Nanostructured metal oxides are promising options for such atmospherically stable semiconductor devices owing to their inherent stability in air. Among various oxide nanostructures, ZnO nanowires have been the most intensively studied for electrical and optical device applications. Here, we demonstrate a strategy for achieving the atmospheric electrical stability of ZnO nanowire devices. Although the chemically active oxygen and water in air are strong candidates for affecting the electrical stability of nanoscale metal oxides, we found that the ppm-level redox-inactive CO_2 in air critically determines the atmospheric electrical stability of hydrothermally grown single-crystalline ZnO nanowires. A series of analyses using atmosphere-controlled electrical characterization of single nanowire devices, Fourier transform infrared spectroscopy, scanning transmission electron microscopy, and X-ray photoelectron spectroscopy consistently revealed that atmospheric CO_2 reacts substantially with the ZnO nanowire surfaces, even at room temperature, to form an electrically insulative zinc carbonate thin layer. The formation of this layer essentially limits the atmospheric electrical stability of the ZnO nanowire devices. Based on this surface carbonation mechanism, we propose a strategy to suppress the detrimental surface reaction, which is based on (1) reducing the density of surface hydroxyl groups and (2) improving the nanowire crystallinity by thermal pretreatment. This approach improves the atmospheric electrical stability to at least 40 days in air.

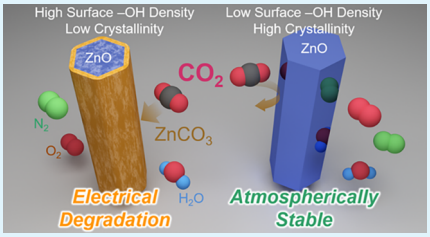

KEYWORDS: *ZnO nanowires, hydrothermal synthesis, long-term stability, zinc carbonate, interface electrical properties, contact resistance*

INTRODUCTION

Recently, the so-called "interactive electronics" have emerged that collect diverse physical and chemical information regarding their surroundings for long periods. The collected space- and time-series data are then analyzed to understand inherently complex phenomena such as disease development, metabolism, and the atmospheric environment.[1−5] Long-term data collection is an essential requirement for this approach.[6,7] Accordingly, the design of atmospherically robust and stable electronic materials is a newly emerging research topic since conventional electronic materials have traditionally been developed and designed in the presence of passivation.[8−11] For example, passivation layers are not applicable to devices such as chemical sensors, which must be exposed to the surroundings, e.g., ambient air.[1,5,12,13] The inherent stability of metal oxide nanostructures in air makes them promising candidates for such atmospherically stable electronic devices. Among various metal oxide nanostructures, single-crystalline ZnO nanowires have gained significant attention due to their attractive electrical and optical properties and the abundance of resources required for their fabrication.[14] Therefore, atmospheric electrical stability of ZnO nanowire devices is an essential subject for a long-term big data correction achieved by utilizing chemical sensors,[15] UV detectors,[16] force/pressure sensors,[17] and energy-harvesting generators.[18] ZnO nanostructures are relatively reactive to both acids and bases,[19] and during their preservation in air, oxygen and water have been considered to have the most effect on their physical properties due to their chemical reactivity.[20−22] In addition, oxygen vacancies in the crystal, which react with oxygen and water in air, are widely recognized as electron donors in binary metal oxides such as ZnO, SnO_2, and others; the formation/compensation of oxygen vacancies generates/eliminates mobile electrons.[23−27] Other species in air are relatively inactive or low in content and have been considered to interact with metal oxide surfaces only under more reactive conditions such as high temperatures.[28,29] Since the electrical properties of nanostructures are inherently affected by many factors, including their interfaces and surfaces,[30] achieving the atmospheric electrical stability of single-crystalline ZnO

Received: July 26, 2019
Accepted: October 4, 2019
Published: October 4, 2019

DOI: 10.1021/acsami.9b13231
ACS Appl. Mater. Interfaces 2019, 11, 40260−40266

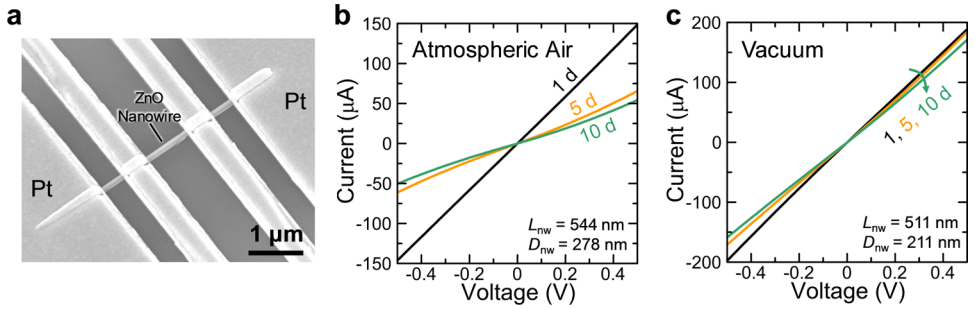

Figure 1. (a) FESEM image of a typical four-terminal ZnO nanowire device. Two-probe *I*−*V* characteristics of ZnO nanowire devices preserved in (b) atmospheric air and (c) vacuum (<10 Pa) conditions at room temperature for 1, 5, and 10 days.

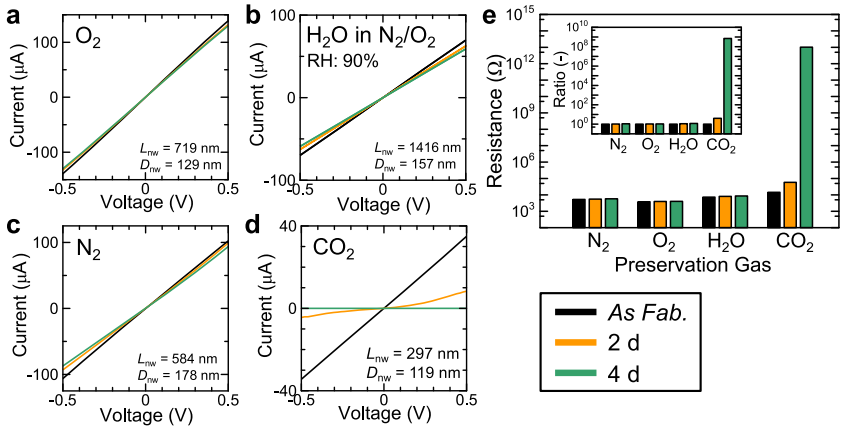

Figure 2. Two-probe *I*−*V* characteristics of ZnO nanowire devices preserved in (a) O_2, (b) H_2O vapor (90% RH in a mixture of N_2 and O_2, N_2/O_2 = 4:1), (c) N_2, and (d) CO_2 atmospheres at room temperature for 0 (immediately after fabrication, shown as "*As Fab.*"), 2, and 4 days. (e) Two-probe resistances of ZnO nanowire devices extracted from the *I*−*V* characteristics in panels (a)−(d). The two-probe resistances normalized by the initial values (*As Fab.*) are shown as "Ratio" in the inset.

nanowires remains a challenging issue for their device application to interactive electronics in air.

Here, we demonstrate a strategy to accomplish the atmospheric electrical stability of ZnO nanowire devices. Although chemically active oxygen and water in air are strong candidates for affecting the long-term electrical stability of nanoscale metal oxides, we found that the ppm-level redox-inactive CO_2 in air critically determines the long-term atmospheric electrical stability of hydrothermally grown single-crystalline ZnO nanowires. A series of analyses revealed that atmospheric CO_2 reacts substantially with the ZnO nanowire surfaces, even at room temperature, to form an electrically insulative zinc carbonate thin layer. The formation of this layer essentially limits the long-term electrical stability of ZnO nanowire devices. Based on this surface carbonation mechanism, we propose a strategy to suppress the detrimental surface reaction, which is based on (1) reducing the density of surface hydroxyl groups and (2) improving the nanowire crystallinity by thermal pretreatment. This approach improves the atmospheric electrical stability to at least 40 days in air.

RESULTS AND DISCUSSION

First, we examined the atmospheric electrical stability of hydrothermally grown single-crystalline ZnO nanowires. The current−voltage (*I*−*V*) characteristics of single ZnO nanowire devices were measured as a function of time during preservation, and a field-emission scanning electron microscope (FESEM) image of the fabricated device is shown in Figure 1a. Figure 1b shows the temporal changes in the two-probe *I*−*V* characteristics of ZnO nanowire devices preserved in atmospheric air at room temperature for 10 days. The measured current values decreased significantly within several days, indicating the instability and electrical degradation of the ZnO nanowire devices in atmospheric air at room temperature. The *I*−*V* curve exhibited nonlinear, or non-Ohmic, characteristics only 5 days after fabrication. Figure 1c shows the temporal changes in the *I*−*V* characteristics of ZnO nanowire devices preserved under vacuum conditions (<10 Pa). Compared with air preservation, preservation under vacuum conditions did not cause significant temporal changes to the *I*−*V* characteristics of the ZnO nanowire devices. This clear difference between the effects of atmospheric air and vacuum conditions during preservation indicates that molecules in air are closely correlated to the observed electrical changes in the ZnO nanowire devices.

Next, we investigated which molecular component of air mainly affects the electrical properties of ZnO nanowire devices at room temperature during preservation. First, we focused on the effects of oxygen and water in air on the measured electrical properties. This is because their chemical reactivities are relatively high compared with the other components of air (N_2, Ar, and CO_2).[20] The temporal changes in the *I*−*V* characteristics of the ZnO nanowire devices preserved under pure oxygen or high-humidity (RH 90%) atmospheres are shown in Figure 2a,b. Contrary to our initial speculations, the oxygen and high-humidity atmospheres did not significantly alter the electrical properties of the ZnO nanowire devices. Note that preservation in a relatively inert

DOI: 10.1021/acsami.9b13231
ACS Appl. Mater. Interfaces 2019, 11, 40260−40266

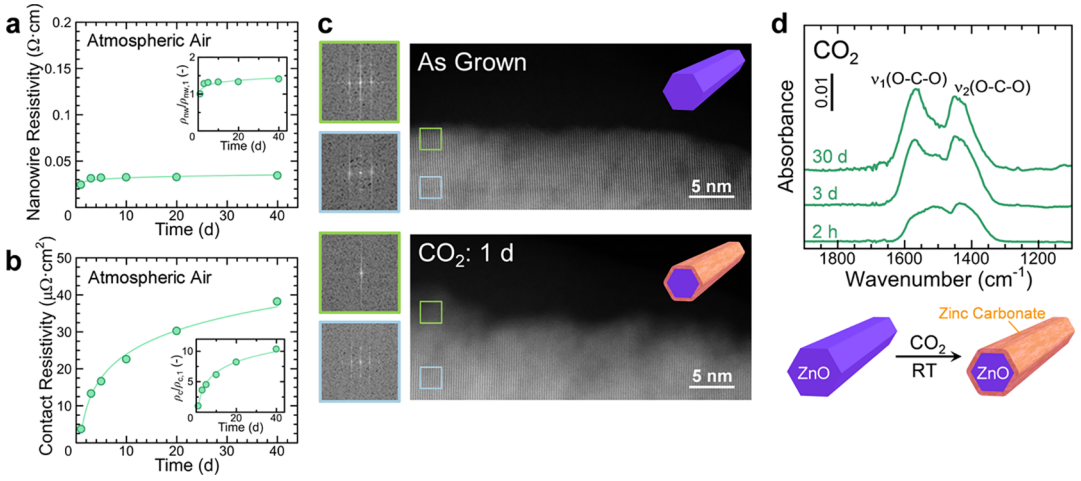

Figure 3. Atmospheric air preservation time dependence of (a) nanowire resistivity and (b) contact resistivity of the ZnO nanowires measured by the four-probe technique. Plotted data are averaged values of three devices. The nanowire resistivity and contact resistivity normalized by those of the first day ($\rho_{nw,1}$ and $\rho_{c,1}$) are shown in the insets. Approximate curves are shown as visual guides. (c) STEM images of the ZnO nanowire surfaces immediately after hydrothermal growth (as grown) and preserved in a CO_2 atmosphere for 1 days. Fast Fourier transform patterns of the surface and core regions (boxed areas) are also shown. (d) FT-IR spectra of ZnO nanowires preserved in a CO_2 atmosphere for 2 h, 3 days, and 30 days.

N_2 atmosphere also did not change their electrical properties, as shown in Figure 2c. The slight degradation in the $I-V$ characteristics in Figure 2a−c is attributed to residual air molecules in the storage box (backpressure <10 Pa) because the same effect was also observed in the time-series analysis under vacuum conditions (Figure 1c). The remaining possible influencing component in air is chemically inactive, ppm-level atmospheric CO_2. The effect of CO_2 preservation on the electrical properties of ZnO nanowire devices is shown in Figure 2d, which clearly illustrates that CO_2 preservation substantially increased the electrical resistance within 2 days. Figure 2e shows a comparison between the effects of different components of air on the electrical resistance of ZnO nanowire devices during preservation. Clearly, the electrical change induced by CO_2 preservation is much greater than the changes caused by the other components. These results reveal that the ppm-level CO_2 in air mainly causes the electrical degradation of ZnO nanowire devices (Figure 1b). Although previous studies on the chemical reaction between CO_2 and ZnO have reported structural analyses under relatively reactive conditions such as high temperatures,[29,31] the present results in Figure 2 imply that atmospheric CO_2 interacts with the ZnO nanowire surfaces even at room temperature, resulting in the observed electrical change. Therefore, the atmospheric stability of the electrical properties of hydrothermal ZnO nanowire devices in air at room temperature is mainly governed by redox-inactive, ppm-level CO_2 rather than by chemically active and high-content oxygen and water.

Since the above results indicate the occurrence of a reaction between atmospheric CO_2 and the ZnO nanowire surface at room temperature, we examined the surface microstructures of ZnO nanowires upon exposure to the air to understand the mechanism of electrical degradation during preservation. Figure 3a,b shows the temporal changes in both nanowire resistivity and contact resistivity (defined as the interface resistivity between nanowires and electrodes normalized by the contact area) obtained by performing four-probe measurements of the ZnO nanowire devices. The nanowire resistivity changed by less than 50% during the 40 days measurements. On the other hand, the contact resistivity increased significantly, by more than 10 times, during the same measurement period. Thus, either the entire nanowire surface or the contact interface between the Pt electrode and nanowire is electrically degraded by CO_2. Therefore, we analyzed the ZnO nanowire surface microstructures by scanning tunneling electron microscopy (STEM) analysis. Figure 3c shows the STEM images of two ZnO nanowires, which are (1) a nanowire immediately after hydrothermal growth (as grown) and (2) a nanowire after preservation in a CO_2 atmosphere for 1 days. For the as-grown nanowire, a single-crystalline structure was observable in the entire region from the core to the surface. On the other hand, for the CO_2-preserved nanowire, a several-nanometer-thick amorphous layer was clearly present on the surface. The surface layer was further investigated by Fourier transform infrared (FT-IR) spectroscopic analysis; Figure 3d shows the FT-IR spectrum of the CO_2-preserved ZnO nanowires. A set of IR peaks appeared at approximately 1400−1600 cm^{-1} during CO_2 preservation, which can be assigned to the vibrations of the carbonate structure (O−C−O) on metal oxides.[32,33] Based on these analyses, we conclude that the formation of an insulative zinc carbonate thin layer on the ZnO nanowire surfaces severely degrades the electrical stability of the device in atmospheric air at room temperature. Since the thickness of zinc carbonate (<5 nm) is much smaller than the nanowire diameter (100−200 nm), electrically conductive cross-sectional area of nanowire, which determines nanowire resistivity, does not change significantly even after the carbonation. On the other hand, contact resistance is directly affected by the thin-surface carbonate layer because contact resistance is a resistance between electrodes and nanowires. Electrical current from electrodes must cross the insulative layer, resulting in a significant increase in contact resistance after carbonation. Note that the nonlinear increase in the resistance of ZnO nanowire device in a CO_2 atmosphere (Figure 2e) could be explained on the basis of a nonlinear nature of tunneling current through an insulative layer. When the direct tunneling process is assumed for a current flow through the insulative

DOI: 10.1021/acsami.9b13231
ACS Appl. Mater. Interfaces 2019, 11, 40260−40266

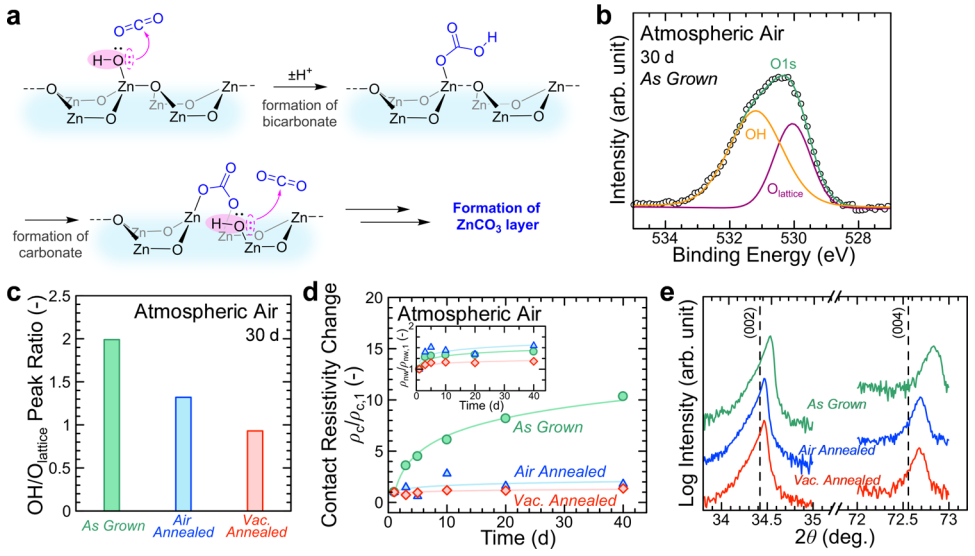

Figure 4. (a) Possible scheme of −OH-promoted carbonate formation on ZnO. (b) XPS O 1s core-level spectrum of as-grown ZnO nanowires preserved in atmospheric air for 30 days. The data are decomposed into two Gaussian peaks originating from surface −OH and lattice oxygen ($O_{lattice}$) of ZnO. (c) XPS peak area ratios between decomposed −OH and $O_{lattice}$ peaks for as-grown, air-annealed, and vacuum-annealed ZnO nanowires preserved in atmospheric air for 30 days. Both air and vacuum (<1.0×10^{-3} Pa) annealing were performed at 600 °C for 1 h. (d) Ambient air preservation time dependence of relative changes in contact resistivity of as-grown, air-annealed, and vacuum-annealed ZnO nanowires measured by four-probe technique. Nanowire resistivity, which corresponds to contact resistivity, is shown in the inset. The data were normalized using the nanowire resistivity and contact resistivity of the first day ($\rho_{nw,1}$ and $\rho_{c,1}$). The plotted data of as-grown and vacuum-annealed ZnO nanowires are averaged values of three and four devices, respectively. Approximate curves are shown as visual guides. (e) XRD patterns of as-grown, air-annealed, and vacuum-annealed ZnO nanowires.

layer, tunneling resistance, which corresponds to contact resistance, exponentially increases as the thickness of zinc carbonate layer increases. In this case, the resistance of ZnO nanowire devices exponentially increases even if the zinc carbonate layer linearly grows as time goes by. Thus, the zinc carbonate layer severely affects the electrical properties of the nanowire devices through the increase in contact resistance because interfacial properties have become increasingly important in nanostructured devices.[30,34]

As discussed above, controlling the formation of zinc carbonate on the surface is essential to improving the atmospheric stability of ZnO nanowire devices in ambient conditions. Based on the formation mechanism of surface zinc carbonate, we assumed that the surface −OH groups play a crucial role. This is because a dangling −OH is favorable for nucleophilically attacking a CO_2 molecule to form a bicarbonate ion. The dangling −OH is regenerated in the process of carbonation ($ZnO + CO_2 \rightarrow ZnCO_3$) to satisfy the reaction material balance and considered to attack another CO_2 (Figure 4a). In fact, it has been reported that CO_2 adsorption on metal oxides is drastically accelerated on −OH-rich surfaces.[32,35,36] Thus, controlling the amount of surface −OH groups is a promising approach to suppressing zinc carbonate formation on ZnO nanowires. Here, we employed a thermal treatment for this purpose because we recently found that thermal pretreatments significantly alter the density of surface −OH groups on ZnO nanowires.[37] Figure 4b shows the O 1s core-level X-ray photoelectron spectroscopy (XPS) spectrum of the as-grown ZnO nanowires, and Figure 4c shows the XPS peak area ratios between the decomposed −OH and lattice oxygen ($O_{lattice}$) peaks for the as-grown, air-annealed, and vacuum-annealed ZnO nanowires preserved in atmospheric air for 30 days. The density of the surface −OH groups was evaluated as the ratio between the two decomposed peak areas that originate from the −OH and $O_{lattice}$ of ZnO.[38,39] In this study, we performed thermal annealing either under atmospheric air or vacuum (<1.0×10^{-3} Pa) conditions at 600 °C for 1 h. Clearly, the peak area intensity of surface −OH groups in the XPS spectra decreased for the annealed samples. This decreased peak area ratio for the annealed ZnO nanowires indicates that both thermal pretreatments reduced the surface −OH density. It was also confirmed that the −OH-reduced surface was maintained for at least 30 days in atmospheric air at room temperature. Figure 4d shows the temporal changes in nanowire resistivity and contact resistivity of (1) as-grown, (2) air-annealed, and (3) vacuum-annealed ZnO nanowire devices during preservation in atmospheric air at room temperature. Note that, for these devices, the ZnO nanowires were annealed immediately after hydrothermal growth and then dropped on the substrate for subsequent electrode patterning. The significant increase in electrical contact resistance, which is the major cause of the electrical instability of as-grown nanowire devices, was strongly suppressed in the annealed nanowire devices. Therefore, the annealing treatment is effective for improving the atmospheric electrical stability of ZnO nanowire devices. In these experiments, the measurements were stopped after 40 days because of two reasons: (1) the stability of the annealed nanowire devices was clearly improved compared with that of the as-grown nanowire device after 40 days and (2) the electrical degradation of the as-grown nanowire device tends to saturate after 40 days. Since 40 days is not a limitation on the electrical stability of the annealed nanowire devices, the robust electrical characteristic could maintain beyond 40 days. However, the surface modification of −OH groups alone cannot explain the effect of thermal annealing on the electrical properties because the effect of a change in only the surface groups is almost negligible on the measurable electrical current through contacts including

DOI: 10.1021/acsami.9b13231
ACS Appl. Mater. Interfaces 2019, 11, 40260−40266

electron tunneling effects. Figure 4e shows the X-ray diffraction (XRD) patterns of the as-grown and annealed nanowires. For the annealed nanowires, the XRD peaks corresponding to ZnO were close to those of pure ZnO,[40,41] indicating that the crystallinity of the as-grown ZnO nanowires was improved by the thermal pretreatments. The smaller full width at half-maximum values of the annealed nanowires support the improvement in crystallinity (see the Supporting information Table SI). Importantly, this improvement to the crystallinity is effective for suppressing ZnO carbonation because the formation of chemical compounds between molecules and solids is generally enhanced in lower-crystallinity solid structures, e.g., the thermal oxidation rate of amorphous/polycrystalline and single-crystalline silicon.[42] These results imply that a cooperative effect of reducing surface −OH density (to prevent CO_2 hydration) and improving crystallinity (to inhibit deeper corrosion by carbonation) by thermal annealing effectively improves the atmospheric electrical stability of ZnO nanowire devices.

CONCLUSIONS

In conclusion, we have demonstrated a strategy to accomplish the atmospheric electrical stability of ZnO nanowire devices. Although the chemically active oxygen and water in air are strong candidates for affecting the electrical stability of nanoscale metal oxides, we found that redox-inactive CO_2 at ppm levels in air critically determines the atmospheric stability of the electrical properties of hydrothermally grown single-crystalline ZnO nanowires. A series of analyses using atmosphere-controlled electrical characterizations of single nanowire devices, FT-IR, STEM, and XPS consistently revealed that atmospheric CO_2 reacts significantly with ZnO nanowire surfaces, even at room temperature, to form an electrically insulative zinc carbonate thin layer. The formation of this layer essentially limits the atmospheric electrical stability of the ZnO nanowire devices. Based on this surface carbonation mechanism, we proposed a strategy to suppress the detrimental surface reaction, which is based on (1) reducing the density of surface −OH groups and (2) improving the nanowire crystallinity by thermal pretreatment. This approach improved the atmospheric electrical stability of the devices to up to 40 days in air.

METHODS

ZnO Nanowire Growth. Single-crystalline ZnO nanowires were hydrothermally grown on a ZnO seed layer/SiO_2/p-Si substrate.[14,43] A 5 nm Ti adhesion layer and 50 nm ZnO seed layer were sequentially deposited onto a 100 nm SiO_2/p-type Si substrate by radio frequency (RF) sputtering. The solution for hydrothermal reactions was a mixture of 25 mM zinc nitrate hexahydrate (Wako, 99.0%), 25 mM hexamethylenetetramine (Wako, 99.0%), and 2.5 mM branched polyethyleneimine (M_n = 1800, Aldrich, 50 wt % in H_2O). The ZnO-deposited substrate was immersed into the growth solution and maintained at 95 °C for 48 h. Until the end of the hydrothermal synthesis, the solution was exchanged with newly prepared solution every 24 h. A ZnO nanowire array was obtained on the substrate after the reaction. For air-annealed or vacuum-annealed devices, the ZnO nanowires were annealed immediately after synthesis for 1 h at 600 °C in atmospheric air or vacuum ($<1.0 \times 10^{-3}$ Pa) conditions, respectively. The standard annealing temperature of 600 °C was set on the basis of the ZnO nanowire characterizations with various annealing temperatures (Supporting Information Figure S1).

Device Fabrication. The hydrothermally grown ZnO nanowires were dispersed in 2-propanol by sonication, then dropped onto a 100 nm SiO_2/n+-type Si substrate with a 5 nm Ti adhesion layer/200 nm Pt pad electrodes, which were patterned by electron beam (EB) lithography and RF sputtering. EB lithography was then performed to fabricate electrical contacts on the dropped nanowires. An EB resist (ZEON, ZEP520A-7) was coated using a spin coater (MIKASA, MS-A100), followed by EB exposure (Elionix) and development (ZEON, ZED-N50). A 250 nm layer of Pt was then deposited by RF sputtering (SEINAN) in an Ar 0.3 Pa atmosphere. Lift-off (*N*,*N*-dimethylformamide) and acetone cleaning processes completed the device fabrication.

Atmosphere-Controlled Preservation Experiments. For the experiments under controlled preservation times and atmospheres, fabricated devices or ZnO nanowire array substrates were placed in a sealed storage box for predetermined intervals between each characterization. For the N_2 (purity 6N), O_2 (purity 6N), H_2O vapor (90% RH in a mixture of N_2 and O_2, N_2/O_2 = 4:1, purity >99%), and CO_2 (purity >95%) preservation experiments, the storage box with samples was evacuated to 10 Pa before gas filling to remove residual ambient air. For the H_2O vapor preservation experiments, the mixture of N_2 and O_2 was introduced into the storage box through a bubbler with deionized water. The RH of the H_2O vapor gas was controlled by dilution after bubbling. All samples were preserved at room temperature.

Electrical Characterization of Nanowire Devices. The two- and four-probe *I*−*V* characteristics of the ZnO nanowire devices were measured using a semiconductor parameter analyzer (Keithley, 4200SCS) with a probe station at room temperature. Nanowire resistivity (ρ_{nw}) and contact resistivity (ρ_c) were extracted from the four-probe measurements of the four-terminal devices. ρ_{nw} was calculated by assuming a circular nanowire cross section: $\rho_{nw} = \pi R_4 D_{nw}^2/(4L_{nw})$, where R_4, D_{nw}, and L_{nw} are the four-probe resistance, nanowire diameter, and length between the two voltage electrodes of each four-terminal device, respectively. ρ_c was calculated as an area-normalized contact resistivity: $\rho_c = 2\pi D_{nw} L_c (R_2 - R_4)$, where R_2 and L_c are the two-probe resistance and length of contact electrodes on the nanowires, respectively. The dimensions of the ZnO nanowires and electrodes were determined using a field-emission scanning electron microscope (FESEM, JEOL, JSM-7610F).

Nanowire Characterizations. The STEM images were obtained by an annular dark field detector with an accelerating voltage of 200 kV and a probe convergence semiangle of 22 mrad. The observed nanowires were dispersed in ethanol and then dropped onto holey carbon films. The FT-IR spectra of the ZnO nanowire arrays were measured using an FT-IR spectrometer (Thermo Fisher Scientific, Nicolet iS50) equipped with a mercury−cadmium−telluride detector. For FT-IR experiments, a double-polished p−-float-zone Si substrate was used for the ZnO nanowire array samples. The FT-IR spectra of the ZnO nanowire arrays immediately after growth or annealing were used as background spectra to evaluate spectral changes attributable to preservation. XPS (Shimadzu/Kratos, AXIS ULTRA, 12 kV, 5 mA, Al Kα X-radiation (1486.6 eV)) was performed to analyze the surface characteristics of the ZnO nanowires. In the XPS experiments, the binding energy was calibrated using the C 1s core level of the C−C bond as 285.0 eV. Structural characterizations of ZnO nanowires were determined by XRD (PHILIPS, X'Pert MRD 45 kV, 40 mA) and FESEM.

ASSOCIATED CONTENT

Supporting Information

The Supporting Information is available free of charge on the ACS Publications website at DOI: 10.1021/acsami.9b13231.

XRD analyses of as-grown and annealed zno nanowires; effect of annealing temperature on characteristics of ZnO nanowires (PDF)

AUTHOR INFORMATION

Corresponding Authors

*E-mail: takahashi.t@cm.kyushu-u.ac.jp (T.T.).
*E-mail: yanagida@cm.kyushu-u.ac.jp (T.Y.).

DOI: 10.1021/acsami.9b13231
ACS Appl. Mater. Interfaces 2019, 11, 40260−40266

ORCID

Tsunaki Takahashi: 0000-0002-2840-8038
Takuro Hosomi: 0000-0002-5649-6696
Kazuki Nagashima: 0000-0003-0180-816X
Naoya Shibata: 0000-0003-3548-5952
Takeshi Yanagida: 0000-0003-4837-5701

Notes

The authors declare no competing financial interest.

■ ACKNOWLEDGMENTS

This work was supported by KAKENHI (grant nos. JP17H04927, JP18H01831, JP18H05243, and JP18KK0112). T.Y. was supported by ImPACT Program of Council for Science, Technology and Innovation (Cabinet Office, Government of Japan). T.T., T.H., K.N., and T.Y. were supported by JST CREST, Japan (grant no. JPMJCR1331). T.Y. and K.N. were supported by CAS-JSPS Joint Research Projects (grant no. JPGJHZ1891). T.T. was supported by Ozawa and Yoshikawa Memorial Electronics Research Foundation. The TEM analysis of this work was supported by "Nanotechnology Platform" (project no. 12024046) of the Ministry of Education, Culture, Sports, Science and Technology (MEXT), Japan. This work was performed under the Cooperative Research Program of "Network Joint Research Center for Materials and Devices" and the MEXT Project of "Integrated Research Consortium on Chemical Sciences". The authors are indebted to Dr. Y. Miura, the Center of Advanced Instrumental Analysis, Kyushu University for the XPS analysis.

■ REFERENCES

(1) Peng, G.; Tisch, U.; Adams, O.; Hakim, M.; Shehada, N.; Broza, Y. Y.; Billan, S.; Abdah-Bortnyak, R.; Kuten, A.; Haick, H. Diagnosing Lung Cancer in Exhaled Breath Using Gold Nanoparticles. *Nat. Nanotechnol.* **2009**, *4*, 669−673.

(2) Orozco-Solís, R.; Matos, R. J. B.; Lopes de Souza, S.; Grit, I.; Kaeffer, B.; Manhaes de Castro, R.; Bolanos-Jimenez, F. Perinatal Nutrient Restriction Induces Long-Lasting Alterations in the Circadian Expression Pattern of Genes Regulating Food Intake and Energy Metabolism. *Int. J. Obes.* **2011**, *35*, 990−1000.

(3) Peng, R. D.; Bell, M. L. Spatial Misalignment in Time Series Studies of Air Pollution and Health Data. *Biostatistics* **2010**, *11*, 720−740.

(4) Lichtenstein, A.; Havivi, E.; Shacham, R.; Hahamy, E.; Leibovich, R.; Pevzner, A.; Krivitsky, V.; Davivi, G.; Presman, I.; Elnathan, R.; Engel, Y.; Flaxer, E.; Patolsky, F. Supersensitive Fingerprinting of Explosives by Chemically Modified Nanosensors Arrays. *Nat. Commun.* **2014**, *5*, No. 4195.

(5) Tanaka, T.; Hoshino, S.; Takahashi, T.; Uchida, K. Nanoscale Pt Thin Film Sensor for Accurate Detection of PPM Level Hydrogen in Air at High Humidity. *Sens. Actuators, B* **2018**, *258*, 913−919.

(6) Scheffer, M.; Bascompte, J.; Brock, W. A.; Brovkin, V.; Carpenter, S. R.; Dakos, V.; Held, H.; van Nes, E. H.; Rietkerk, M.; Sugihara, G. Early-Warning Signals for Critical Transitions. *Nature* **2009**, *461*, 53−59.

(7) Chen, L.; Liu, R.; Liu, Z.-P.; Li, M.; Aihara, K. Detecting Early-Warning Signals for Sudden Deterioration of Complex Diseases by Dynamical Network Biomarkers. *Sci. Rep.* **2012**, *2*, No. 342.

(8) Zhou, W.; Dai, X.; Fu, T.-M.; Xie, C.; Liu, J.; Lieber, C. M. Long Term Stability of Nanowire Nanoelectronics in Physiological Environments. *Nano Lett.* **2014**, *14*, 1614−1619.

(9) Lim, T.; Bong, J.; Mills, E. M.; Kim, S.; Ju, S. Highly Stable Operation of Metal Oxide Nanowire Transistors in Ambient Humidity, Water, Blood, and Oxygen. *ACS Appl. Mater. Interfaces* **2015**, *7*, 16296−16302.

(10) Hsu, P. C.; Wu, H.; Carney, T. J.; McDowell, M. T.; Yang, Y.; Garnett, E. C.; Li, M.; Hu, L.; Cui, Y. Passivation Coating on Electrospun Copper Nanofibers for Stable Transparent Electrodes. *ACS Nano* **2012**, *6*, 5150−5156.

(11) Hwang, I.; Jeong, I.; Lee, J.; Ko, M. J.; Yong, K. Enhancing Stability of Perovskite Solar Cells to Moisture by the Facile Hydrophobic Passivation. *ACS Appl. Mater. Interfaces* **2015**, *7*, 17330−17336.

(12) Peng, N.; Zhang, Q.; Chow, C. L.; Tan, O. K.; Marzari, N. Sensing Mechanisms for Carbon Nanotube Based NH_3 Gas Detection. *Nano Lett.* **2009**, *9*, 1626−1630.

(13) Meng, G.; Zhuge, F.; Nagashima, K.; Nakao, A.; Kanai, M.; He, Y.; Boudot, M.; Takahashi, T.; Uchida, K.; Yanagida, T. Nanoscale Thermal Management of Single SnO_2 Nanowire: Pico-Joule Energy Consumed Molecule Sensor. *ACS Sens.* **2016**, *1*, 997−1002.

(14) Xu, S.; Wang, Z. L. One-Dimensional ZnO Nanostructures: Solution Growth and Functional Properties. *Nano Res.* **2011**, *4*, 1013−1098.

(15) Wan, Q.; Li, Q. H.; Chen, Y. J.; Wang, T. H.; He, X. L.; Li, J. P.; Lin, C. L. Fabrication and Ethanol Sensing Characteristics of ZnO Nanowire Gas Sensors. *Appl. Phys. Lett.* **2004**, *84*, 3654−3656.

(16) Gedamu, D.; Paulowicz, I.; Kaps, S.; Lupan, O.; Wille, S.; Haidarschin, G.; Mishra, Y. K.; Adelung, R. Rapid Fabrication Technique for Interpenetrated ZnO Nanotetrapod Networks for Fast UV Sensors. *Adv. Mater.* **2014**, *26*, 1541−1550.

(17) Wang, X.; Zhou, J.; Song, J.; Liu, J.; Xu, N.; Wang, Z. L. Piezoelectric Field Effect Transistor and Nanoforce Sensor Based on a Single ZnO Nanowire. *Nano Lett.* **2006**, *6*, 2768−2772.

(18) Fan, F. R.; Tang, W.; Wang, Z. L. Flexible Nanogenerators for Energy Harvesting and Self-Powered Electronics. *Adv. Mater.* **2016**, *28*, 4283−4305.

(19) Atkins, P. W.; Overton, T.; Rourke, J.; Weller, M.; Armstrong, F. *Shriver & Atkins Inorganic Chemistry*; Oxford University Press, W.H. Freeman and Co.: Oxford, New York; New York, 2006.

(20) Schultze, J. W.; Lohrengel, M. M. Stability, Reactivity and Breakdown of Passive Films. Problems of Recent and Future Research. *Electrochim. Acta* **2000**, *45*, 2499−2513.

(21) Sengupta, G.; Ahluwalia, H. S.; Banerjee, S.; Sen, S. P. Chemisorption of Water Vapor on Zinc Oxide. *J. Colloid Interface Sci.* **1979**, *69*, 217−224.

(22) Zhou, J.; Xu, N. S.; Wang, Z. L. Dissolving Behavior and Stability of ZnO Wires in Biofluids: A Study on Biodegradability and Biocompatibility of ZnO Nanostructures. *Adv. Mater.* **2006**, *18*, 2432−2435.

(23) Higuchi, M.; Uekusa, S.; Nakano, R.; Yokogawa, K. Postdeposition Annealing Influence on Sputtered Indium Tin Oxide Film Characteristics. *Jpn. J. Appl. Phys.* **1994**, *33*, 302−306.

(24) Kang, H. S.; Kang, J. S.; Pang, S. S.; Shim, E. S.; Lee, S. Y. Variation of Light Emitting Properties of ZnO Thin Films Depending on Post-Annealing Temperature. *Mater. Sci. Eng., B* **2003**, *102*, 313−316.

(25) Anzai, H.; Takahashi, T.; Suzuki, M.; Kanai, M.; Zhang, G.; Hosomi, T.; Seki, T.; Nagashima, K.; Shibata, N.; Yanagida, T. Unusual Oxygen Partial Pressure Dependence of Electrical Transport of Single-Crystalline Metal Oxide Nanowires Grown by the Vapor−Liquid−Solid Process. *Nano Lett.* **2019**, *19*, 1675−1681.

(26) Anzai, H.; Suzuki, M.; Nagashima, K.; Kanai, M.; Zhu, Z.; He, Y.; Boudot, M.; Zhang, G.; Takahashi, T.; Kanemoto, K.; Seki, T.; Shibata, N.; Yanagida, T. True Vapor−Liquid−Solid Process Suppresses Unintentional Carrier Doping of Single Crystalline Metal Oxide Nanowires. *Nano Lett.* **2017**, *17*, 4698−4705.

(27) Soleimanian, V.; Ghasemi Varnamkhasti, M. Influence of Oxygen Partial Pressure on Opto-Electrical Properties, Crystallite Size and Dislocation Density of Sn Doped In_2O_3 Nanostructures. *J. Electron. Mater.* **2016**, *45*, 5395−5403.

(28) Lu, H.; Reddy, E. P.; Smirniotis, P. G. Calcium Oxide Based Sorbents for Capture of Carbon Dioxide at High Temperatures. *Ind. Eng. Chem. Res.* **2006**, *45*, 3944−3949.

DOI: 10.1021/acsami.9b13231
ACS Appl. Mater. Interfaces 2019, 11, 40260−40266

(29) Sawada, Y.; Murakami, M.; Nishide, T. Thermal Analysis of Basic Zinc Carbonate. Part 1. Carbonation Process of Zinc Oxide Powders at 8 and 13 °C. *Thermochim. Acta* **1996**, *273*, 95−102.
(30) Léonard, F.; Talin, A. A. Electrical Contacts to One- and Two-Dimensional Nanomaterials. *Nat. Nanotechnol.* **2011**, *6*, 773−783.
(31) Pan, Z.; Tao, J.; Zhu, Y.; Huang, J.-F.; Paranthaman, M. P. Spontaneous Growth of $ZnCO_3$ Nanowires on ZnO Nanostructures in Normal Ambient Environment: Unstable ZnO Nanostructures. *Chem. Mater.* **2010**, *22*, 149−154.
(32) Gankanda, A.; Cwiertny, D. M.; Grassian, V. H. Role of Atmospheric CO_2 and H_2O Adsorption on ZnO and CuO Nanoparticle Aging: Formation of New Surface Phases and the Impact on Nanoparticle Dissolution. *J. Phys. Chem. C* **2016**, *120*, 19195−19203.
(33) Shamsipur, M.; Pourmortazavi, S. M.; Hajimirsadeghi, S. S.; Zahedi, M. M.; Rahimi-Nasrabadi, M. Facile Synthesis of Zinc Carbonate and Zinc Oxide Nanoparticles via Direct Carbonation and Thermal Decomposition. *Ceram. Int.* **2013**, *39*, 819−827.
(34) Zeng, H.; Takahashi, T.; Kanai, M.; Zhang, G.; He, Y.; Nagashima, K.; Yanagida, T. Long-Term Stability of Oxide Nanowire Sensors via Heavily Doped Oxide Contact. *ACS Sens.* **2017**, *2*, 1854−1859.
(35) Cheng, J.; Poduska, K. M. Ambient Degradation of ZnO Powders: Does Surface Polarity Matter? *ECS J. Solid State Sci. Technol.* **2014**, *3*, P133−P137.
(36) Deng, W.; Zhang, L.; Li, L.; Chen, S.; Hu, C.; Zhao, Z.-J.; Wang, T.; Gong, J. Crucial Role of Surface Hydroxyls on the Activity and Stability in Electrochemical CO_2 Reduction. *J. Am. Chem. Soc.* **2019**, *141*, 2911−2915.
(37) Wang, C.; Hosomi, T.; Nagashima, K.; Takahashi, T.; Zhang, G.; Kanai, M.; Zeng, H.; Mizukami, W.; Shioya, N.; Shimoaka, T.; Tamaoka, T.; Yoshida, H.; Takeda, S.; Yasui, T.; Baba, Y.; Aoki, Y.; Terao, J.; Hasegawa, T.; Yanagida, T. Rational Method of Monitoring Molecular Transformations on Metal-Oxide Nanowire Surfaces. *Nano Lett.* **2019**, *19*, 2443−2449.
(38) Kunat, M.; Girol, S. G.; Burghaus, U.; Woll, C. The Interaction of Water with the Oxygen-Terminated, Polar Surface of ZnO. *J. Phys. Chem. B* **2003**, *107*, 14350−14356.
(39) Al-Gaashani, R.; Radiman, S.; Daud, A. R.; Tabet, N.; Al-Douri, Y. XPS and Optical Studies of Different Morphologies of ZnO Nanostructures Prepared by Microwave Methods. *Ceram. Int.* **2013**, *39*, 2283−2292.
(40) Wei, X. Q.; Zhang, Z. G.; Liu, M.; Chen, C. S.; Sun, G.; Xue, C. S.; Zhuang, H. Z.; Man, B. Y. Annealing Effect on the Microstructure and Photoluminescence of ZnO Thin Films. *Mater. Chem. Phys.* **2007**, *101*, 285−290.
(41) Kang, H. S.; Kang, J. S.; Kim, J. W.; Lee, S. Y. Annealing Effect on the Property of Ultraviolet and Green Emissions of ZnO Thin Films. *J. Appl. Phys.* **2004**, *95*, 1246−1250.
(42) Kamins, T. I. Structure and Properties of LPCVD Silicon Films. *J. Electrochem. Soc.* **1980**, *127*, 686−690.
(43) He, Y.; Yanagida, T.; Nagashima, K.; Zhuge, F.; Meng, G.; Xu, B.; Klamchuen, A.; Rahong, S.; Kanai, M.; Li, X.; Suzuki, M.; Kai, S.; Kawai, T. Crystal-Plane Dependence of Critical Concentration for Nucleation on Hydrothermal ZnO Nanowires. *J. Phys. Chem. C* **2013**, *117*, 1197−1203.

DOI: 10.1021/acsami.9b13231
ACS Appl. Mater. Interfaces 2019, 11, 40260−40266